ELSEVIER

Journal of Alloys and Compounds 218 (1995) 183–189

Journal of ALLOYS AND COMPOUNDS

Structural and physical properties of $UFe_{10}Mo_2$

A.P. Gonçalves [a], P. Estrela [b], J.C. Waerenborgh [a,c], M. Godinho [b], M. Almeida [a,*], J.C. Spirlet [c]

[a] *Departamento de Química, ICEN-INETI, P-2686 Sacavém Codex, Portugal*

[b] *Departamento de Física, Faculdade de Ciências de Universidade de Lisboa, P-1700 Lisbon, Portugal*

[c] *European Commission, Joint Research Centre, Institute of Transuranium Elements, Postfach 2340, D-76125 Karlsruhe, Germany*

Received 15 July 1994

Abstract

$UFe_{10}Mo_2$ was obtained as single-phase polycrystalline material by annealing at 1450 K a polyphasic sample prepared by melting the elements. This compound was characterized by single-crystal X-ray diffraction, ^{57}Fe Mössbauer spectroscopy and magnetization measurements. $UFe_{10}Mo_2$ was found to crystallize in the space group *I4/mmm* with cell parameters $a = 8.4859(3)$ Å, $c = 4.7508(2)$ Å, $V = 342.103(21)$ Å^3, $Z = 2$ and a $ThMn_{12}$-type structure that was solved by single-crystal X-ray diffraction to a final $R = 0.0345$ ($wR = 0.0372$). The Mo atoms are randomly distributed in the 8*i* positions. Magnetization measurements show a ferromagnetic-like behaviour for $T < 198$ K and, in free powder, a saturation magnetization at low temperature of 8.8 μ_B per formula unit. Comparison with fixed powder measurements indicates a basal plane type of anisotropy. ^{57}Fe Mössbauer spectra below T_c show a distribution of hyperfine fields from 0 to 20 T. This distribution was analysed considering the different local configurations around each Fe atom and assuming the Fe site distribution deduced from X-ray data.

Keywords: Intermetallic compounds; Magnetic properties; Uranium compounds

1. Introduction

Uranium intermetallic compounds with the $ThMn_{12}$-type structure (Fig. 1) have recently received considerable interest [1–4]. The rare earth compounds with this type of structure were extensively studied in the past and are regarded as having a high potential for providing good hard magnetic materials [5,6]. The corresponding uranium compounds, particularly those with iron and general formula UFe_xM_{12-x}, only more recently started to be studied. Among these, $UFe_{10}Mo_2$ was identified as having a $ThMn_{12}$-type structure but was obtained only as a multiphasic material and poorly characterized [7–9].

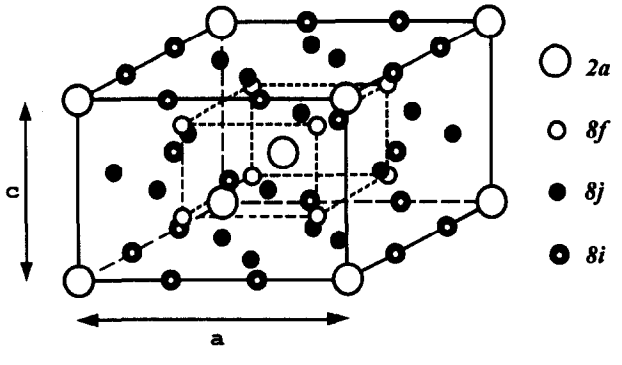

Fig. 1. Unit cell of $ThMn_{12}$-type structure.

As part of a thorough study of the UFe_xM_{12-x} compounds undertaken in this laboratory, we recently obtained $UFe_{10}Mo_2$ as a monophasic material. In this paper we report its study by single-crystal X-ray diffraction, ^{57}Fe Mössbauer spectroscopy and magnetization measurements on single-phase samples.

2. Experimental details

The samples were prepared by induction melting, in a levitation cold crucible, of stoichiometric amounts of the constituent elements (99.9 wt.% purity or better) under vacuum. The ingots were remelted several times in order to ensure perfect homogeneity. Metallographic examination of the solidified molten samples with $UFe_{10}Mo_2$ nominal composition revealed an incongruent

* Corresponding author.

SSDI 0925-8388(94)01403-5

melting character, Fe–Mo and UFe_2 phases being present in addition to the dominant $UFe_{10}Mo_2$ phase with the $ThMn_{12}$-type structure. The prepared samples were wrapped in tantalum foil, sealed in evacuated quartz ampoules and annealed for about 10 days at approximately 1175 °C, followed by rapid cooling to room temperature. This treatment gave a single-phase material of composition $UFe_{10}Mo_2$, which was confirmed by scanning electron microscopy–energy-dispersive spectroscopy (SEM–EDS) analysis, with small amounts of metallic iron which tended to be segregated at the outer surface. Polycrystalline $UFe_{10}Mo_2$ samples almost free from metallic iron were prepared by annealing a material with a slightly different nominal composition, $UFe_{9.5}Mo_{1.5}$. From these samples, single crystals with approximate dimensions of $0.5\times0.5\times0.5$ mm^3 were isolated and the traces of α-iron removed by magnetic separation after grinding.

A grey metallic-looking single crystal ($0.072\times0.072\times0.054$ mm^3) of $UFe_{10}Mo_2$ was extracted from the polycrystalline material, glued on top of a glass fibre and transferred to a goniometer head mounted on an Enraf–Nonius CAD-4 diffractometer equipped with graphite-monochromatized Mo Kα radiation ($\lambda = 0.71073$ Å). The unit cell parameters were obtained by least-squares refinement of the 2θ values of 25 reflections from various regions of the reciprocal space in the range $27° \leqslant 2\theta \leqslant 42°$.

The data set was collected at room temperature in an ω–2θ scan mode ($\Delta\omega = 0.80 + 0.35 \tan\theta$). Two reflections were monitored as intensity and four as orientation standards at 4 h intervals during the data collection; no variation larger than 5% was observed. The intensities of the 2103 measured reflections (with $2\theta < 80°$) were corrected for absorption according to North et al. [10] and for Lorentz and polarization effects. Equivalent reflections were averaged, resulting in 336 unique reflections from which 327 with $I \geqslant 3\sigma(I)$ were considered significant.

The intensity data were consistent with the space group *I4/mmm* and the $ThMn_{12}$-type structure. The structure was refined by the programme UPALS [11]. Scattering factors for neutral atoms as well as anomalous dispersion corrections were taken from Ref. [12]. The extinction coefficient of a type 1 isotropic secondary extinction correction, according to the Becker and Coppens formalism [13,14], was refined together with the scale factor, four isotropic temperature factors, two position parameters (x for 8*j* and 8*i* positions) and three occupation factors; the occupation by Fe and Mo of the 8*f*, 8*j* and 8*i* sites was constrained to vary within the full site occupancy. The least-squares procedure easily converged to the solution where all the Mo atoms are located in the 8*i* sites and with final values of $R = \Sigma|F_{obs} - F_{calc}|/\Sigma|F_{obs}| = 0.0345$ and $wR = 0.0372$ (with $w = 1/\sigma^2(F)$). Crystal data and experimental details of the structure determination are compiled in Table 1. Atomic positions, occupation factors and thermal displacement parameters are presented in Table 2. A refinement made with Fe and Mo free-occupation factors gave essentially the same results, confirming the previous constraint of full site occupancy according to the ideal formula.

Mössbauer absorbers were prepared by crushing monophasic polycrystalline material and pressing the sample powder (about 5 mg cm^{-2} of natural Fe) into a Perspex holder. Mössbauer measurements were performed in transmission mode using a conventional constant-acceleration spectrometer and a 25 mCi ^{57}Co source in an Rh matrix. The velocity scale was calibrated using an α-Fe foil at room temperature. Spectra were obtained at various temperatures in the range 80–300 K. Low temperature measurements were performed using a nitrogen flow cryostat. The spectra (Fig. 2) were fitted to lorentzian peaks using a modified version [16] of the non-linear least-squares computer method of Stone [17]. Several constraints were used as described in the next section.

Magnetization measurements were performed on polycrystalline samples (0.065 g) in the temperature range 5–400 K under fields up to 5 T using a superconducting quantum interference device (SQUID) magnetometer (MPMS Quantum Design). Both free powder and powder fixed with solid paraffin were used as samples.

3. Results and discussion

The single-crystal X-ray structure confirms previous X-ray powder measurements indicating a $ThMn_{12}$-type structure [7]. Furthermore, the present refinement clearly shows that the molybdenum atoms are randomly distributed in the 8*i* positions. Interatomic distances and average numbers of nearest neighbours for the various positions are listed in Table 3.

The occupation of the 8*i* positions by the Mo atoms was already observed by De Mooij and Buschow [18] in the isostructural lanthanide compounds $RFe_{10}Mo_2$ (R, rare earth). This preferential site occupation was explained by the authors considering the contribution of R–Mo, R–Fe and Fe–Mo bonds to the enthalpy of formation of the compound. They showed that the R–Mo pair interactions make a positive contribution and the R–Fe and Fe–Mo bonds a negative one. A preferential occupation of Mo atoms at 8*i* positions minimizes the number of direct R–Mo bonds and maximizes the number of Fe–Mo and R–Fe bonds, leading to the stabilization of the $ThMn_{12}$-type structure. The experimental observation of U_2Mo and $U_{11}Mo_5$ compounds [19] indicates that the U–Mo bonds make a negative contribution to the enthalpy of $UFe_{10}Mo_2$ in spite of theoretical predictions of small but positive

Table 1
Crystal data and details of $UFe_{10}Mo_2$ structure determination

Chemical formula	$UFe_{10}Mo_2$
Formula weight	988.379 g mol^{-1}
Crystal system	Tetragonal
Space group [15]	*I4/mmm* (No. 139)
a	8.4859(3) Å
c	4.7508(2) Å
V	342.103(21) $Å^3$
Z	2
D_{calc}	9.594 g cm^{-3}
μ(Mo Kα)	48.68 cm^2 g^{-1}
Approximate crystal dimensions	$0.07\times0.07\times0.05$ mm^3
Radiation, wavelength	Mo Kα, 0.71073 Å
Monochromator	Graphite
Temperature	295 K
θ range	1.5°–40.0°
ω–2θ scan	$\Delta\omega = 0.80 + 0.35 \tan\theta$
Data set	$-15<h<15$, $-15<k<15$, $-8<l<8$
Crystal-to-receiving-aperture distance	173 mm
Horizontal, vertical aperture	4, 4 mm
Total data	2103
Unique data	336
Observed data ($I \geqslant 3\sigma(I)$)	327
Number of refined parameters	11
Final agreement factors [a]	
$R = \Sigma\|\|F_{obs}\| - \|F_{calc}\|\|/\Sigma\|F_{obs}\|$	0.0345
$wR = [\Sigma(w(\|F_{obs}\| - \|F_{calc}\|)^2)/\Sigma w\|F_{obs}\|^2]^{1/2}$	0.0372
$S = [\Sigma w(\|F_{obs}\| - \|F_{calc}\|)^2/(m-n)]^{1/2}$	0.878

[a] *m*, number of observations; *n*, number of variables.

Table 2
Atomic positions (*x*, *y*, *z*), occupation factors (OF) and temperature factors (*U*) estimated in refinement. The temperature factor is expressed as $T(\theta) = \exp[-8\pi^2 U(\sin\theta/\lambda)^2]$

Atom	Position	*x*	*y*	*z*	OF	$U\times10^2$ (Å^2)
U	2*a*	0	0	0	1	0.49(1)
Fe	8*f*	$\frac{1}{4}$	$\frac{1}{4}$	$\frac{1}{4}$	1.05(4)	0.35(2)
Mo	8*f*	$\frac{1}{4}$	$\frac{1}{4}$	$\frac{1}{4}$	−0.05(4)	0.35(2)
Fe	8*j*	0.2854(2)	$\frac{1}{2}$	0	1.06(5)	0.46(3)
Mo	8*j*	0.2854(2)	$\frac{1}{2}$	0	−0.06(5)	0.46(3)
Fe	8*i*	0.3564(1)	0	0	0.56(5)	0.42(2)
Mo	8*i*	0.3564(1)	0	0	0.44(5)	0.42(2)

formation enthalpies for uranium–molybdenum binary compounds [20]. The contribution of the Fe–Mo bonds to the enthalpy can be neglected since it was experimentally found to be close to zero [21]. Therefore the observed preferential 8*i* occupation of the molybdenum atoms in $UFe_{10}Mo_2$ clearly indicates that the negative U–Fe contribution to the enthalpy is much higher than the U–Mo contribution, the present atomic distribution maximizing the number of U–Fe interactions.

The Mössbauer spectra obtained between room temperature and 200 K show two asymmetrical peaks as seen in Fig. 2. These spectra have the same shape as those published by Suski et al. [22] for $UFe_{10}Si_2$ and $UFe_{10}Si_{1.75}Mo_{0.25}$ at 658 and 588 K respectively, when both compounds are in the paramagnetic state. In our spectra, which show no sign of the presence of α-Fe impurity, the area of the broader peak is approximately 50% higher than the area of the other one. This can be understood in the light of the iron site distribution deduced from our X-ray diffraction results if one assumes that the contribution to the Mössbauer spectra from the Fe atoms in the 8*i* positions is totally under the high velocity peak. The spectra were thus fitted assuming three quadrupole doublets. The linewidths Γ as well as the areas of both peaks in each doublet were constrained to remain equal. The final estimated values for the hyperfine parameters (isomer shifts δ and quadrupole splittings Δ) are given in Table 4.

At 160 K a broad absorption band at the base of the two peaks is already visible (Fig. 2), suggesting the presence of magnetically ordered iron atoms, in good agreement with the magnetic data which indicate a ferromagnetic behaviour for $T<198$ K (see next).

At 80 K the spectrum consists of a very broad absorption band (Fig. 2) and is very similar to that previously published [8] for $UFe_{10}Mo_2$ at 4.2 K. It can be fitted assuming a distribution of magnetic hyperfine fields (B_{hf}) from 0 to about 20 T. Very low fields starting from 0 T (i.e. a quadrupole doublet) had to be considered in this fitting, in contrast with the results published for the isostructural rare earth compounds $RFe_{10}Mo_2$

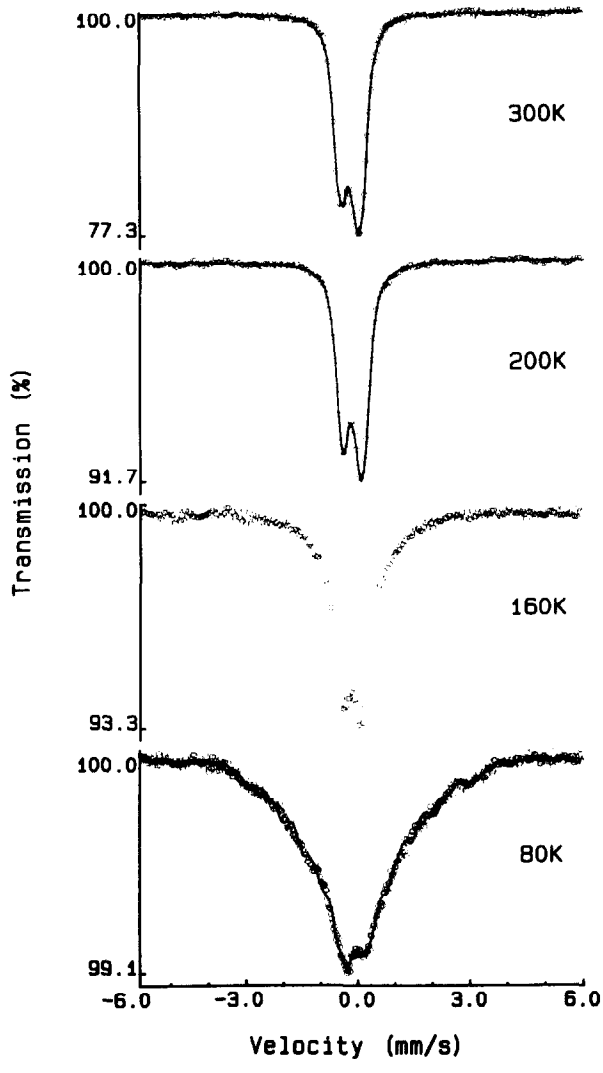

Fig. 2. ^{57}Fe Mössbauer spectra of $UFe_{10}Mo_2$ obtained at various temperatures.

and $RFe_{10}V_2$ [23,24], in which Mo(V) also seems to be present only at the 8*i* sites. Nevertheless, an analysis identical to the one proposed by Sinnemann et al. [23] for $RFe_{10}Mo_2$ was attempted.

According to this method, B_{hf} on an Fe atom depends on the type of crystallographic site on which it is located and on the number of its nearest neighbours. The intensity of each sextet fitted to the spectrum will thus be proportional to the probability of the possible nearest-neighbour configurations of the Fe atoms. Assuming a statistical occupation of the Mo atoms exclusively on the 8*i* sites, the probability of finding *m* nearest Mo neighbours in a shell of *n* nearest-neighbour 8*i* atoms is given by the binomial distribution function

$$P_n(m) = \frac{n!}{m!(n-m)!} x^m (1-x)^{n-m}$$

where $x = 0.5$ is the relative atomic fraction of Mo atoms occupying the 8*i* sites. The relative intensities of each subspectrum calculated from these probabilities are the same as those given for $RFe_{10}V_2$ in Ref. [25].

For simplicity, subspectra with relative intensities lower than 3% were not considered and therefore only 10 subspectra were fitted: nine magnetic splittings and one quadrupole doublet (corresponding to $B_{hf} \approx 0$ T). The width of the Lorentz quadrupole lines was kept fixed at 0.40 mm s^{-1}; the areas of the two peaks of the quadrupole doublet were considered equal and the intensity ratios within each magnetic splitting (I_2/I_1 and I_3/I_1) were kept the same. In order to be able to fit the spectrum, the replacement of an iron nearest neighbour by Mo had to reduce the B_{hf} of Fe at the 8*i* sites by about 15% and even more in the case of Fe at the other sites. Differences in these assumptions and those used in the analysis of the $RFe_{10}Mo_2$ spectra [23] arise from the fact that for $UFe_{10}Mo_2$, as already mentioned, the absorption is the highest for Doppler velocities close to the centre of gravity of the spectrum, in contrast with the rare earth compound spectra. The values estimated for the average hyperfine parameters (isomer shift $\bar{\delta}$, quadrupole shift $\bar{\epsilon}$ as defined in Ref. [26], quadrupole doublet $\bar{\Delta}$, magnetic hyperfine field $\bar{B}_{hf}$) in the best fit are given in Table 5. The corresponding average Fe moments $\bar{\mu}$ were calculated using a hyperfine interaction constant of 14.5 T μ_B^{-1} [26]. The resulting

Table 3
Interatomic distances (*d*) and average numbers of nearest neighbours (NN) of $UFe_{10}Mo_2$

	NN	Atoms	*d*		NN	Atoms	*d*
U(2*a*)–	8	Fe(8*f*)	3.227(0)	Fe(8*f*)–	2	Fe(8*f*)	2.375(0)
	8	Fe(8*j*)	2.993(1)		4	Fe(8*j*)	2.450(1)
	4	(Fe, Mo)(8*i*)	3.024(1)		4	(Fe, Mo)(8*i*)	2.594(1)
					2	U(2*a*)	3.227(0)
Fe(8*j*)–	4	Fe(8*f*)	2.450(1)	(Fe, Mo)(8*i*)–	4	Fe(8*f*)	2.594(1)
	2	Fe(8*j*)	2.575(2)		2	Fe(8*j*)	2.663(2)
	2	(Fe, Mo)(8*i*)	2.663(2)		2	Fe(8*j*)	2.711(2)
	2	(Fe, Mo)(8*i*)	2.711(2)		1	(Fe, Mo)(8*i*)	2.437(2)
	2	U(2*a*)	2.993(1)		4	(Fe, Mo)(8*i*)	2.935(1)
					1	U(2*a*)	3.024(1)

Table 4
Hyperfine parameters[a] estimated from the Mössbauer spectra of $UFe_{10}Mo_2$ at various temperatures T above 198 K

T (K)	Site	δ (mm s^{-1})	Δ (mm s^{-1})	I (%)
300	8*i*	−0.10	0.13	20
	8*j*	−0.18	0.67	40
	8*f*	−0.20	0.44	40
260	8*i*	−0.10	0.13	20
	8*j*	−0.16	0.73	40
	8*f*	−0.16	0.40	40
240	8*i*	−0.07	0.14	20
	8*j*	−0.15	0.69	40
	8*f*	−0.15	0.43	40
200	8*i*	−0.04	0.17	20
	8*j*	−0.12	0.70	40
	8*f*	−0.14	0.43	40

[a] δ, isomer shift relative to α-Fe; Δ, quadrupole splitting; estimated standard deviations in δ and Δ are 0.01 mm s^{-1} or less.

Table 5
Average hyperfine parameters[a] of $UFe_{10}Mo_2$ estimated from Mössbauer spectra at 80 K

Site	$\bar{\delta}$ (mm s^{-1})	Δ (mm s^{-1})	$\bar{\epsilon}$ (mm s^{-1})	$\bar{B}_{hf}$ (T)	$\bar{\mu}$ (μ_B)	I (%)
8*i*	0.031	–	0.067	16.0	1.1	20
8*j*	−0.041	–	0.088	8.9	0.6	40
8*f*	−0.056	0.40[b]	0.000	3.1	0.2	40

[a] $\bar{\delta}$, average isomer shift relative to α-Fe; Δ, quadrupole splitting; $\bar{\epsilon}$, average quadrupole shift; B_{hf}, average magnetic hyperfine field; $\bar{\mu}$, estimated magnetic moment of the Fe atoms assuming $\mu = 14.5$ T μ_B^{-1}; I, relative area kept fixed during fitting, calculated from the probability of the possible nearest-neighbour configurations for each site;

[b] value estimated from the quadrupole doublet corresponding to the $B_{hf} = 0$ T component of the distribution.

curve, shown by the full line plotted on the 80 K spectrum of Fig. 2, is in excellent agreement with the experimental points.

In agreement with the results published for $UFe_{10}Si_2$ [27] and the rare earth compounds [24], the B_{hf} value at the 8*i* sites appears to be the largest. Since the total intensity of the subspectra and the statistics of the Mo nearest neighbours are identical for the 8*f* and 8*j* sites, an assignment of the two sets of lower B_{hf} to these sites is not possible from the experimental results only. The assignments for these two sites in Tables 4 and 5 were done according to what was found for $UFe_{10}Si_2$ [27] and the analogous rare earth compounds [24]. The similarity between the quadrupole splitting Δ estimated for the fitted doublet in the 80 K spectrum and that estimated for one of the quadrupole doublets fitted to the spectra obtained above the Curie temperature ($T_c = 198$ K) seems to confirm that the Fe atoms with the lowest B_{hf}, as well as those which remain paramagnetic at 80 K, are only present at one of the sites 8*f* or 8*j*. According to previous experimental results [24,28–30] and theoretical band calculations [31,32] performed for isostructural rare earth compounds, $\mu_{Fe}(8j) > \mu_{Fe}(8f)$, which supports the assumption that the paramagnetic atoms are located in the 8*f* positions. The observed average Fe–Fe distances d_{FeFe} are in agreement with this picture, following the relation $d_{FeFe}(8i) > d_{FeFe}(8j) > d_{FeFe}(8f)$ (Table 3).

The temperature dependence of the magnetization M measured under various magnetic fields, both upon warming after zero-field cooling (ZFC) and after cooling in the measurement field (FC), is shown in Fig. 3. The $M(T)$ dependence shows a ferromagnetic-like behaviour with a critical temperature T_c of 198 ± 2 K, above which a Curie–Weiss law with $\theta = 198(2)$ K is followed. The ZFC and FC curves show an irreversible behaviour for temperatures below T_c, while the $M(H)$ curves exhibit a small hysteresis, easily reaching saturation for the lower temperatures. The coercive field at 10 K is less than 500 Oe and the remanence is about 1.6 μ_B per formula unit (f.u.).

The $M(H)$ dependence at various temperatures for fields up to 5.5 T is shown in Fig. 4. The linear dependence verified in the highest fields, which corresponds to a saturated magnetization (M_s) or an approximation to saturation, enables one to obtain the temperature dependence of the "spontaneous magnetization" M_0 by linear extrapolation of $M(H \rightarrow 0)$ at each temperature. From the dependence $M_0(T)$ the

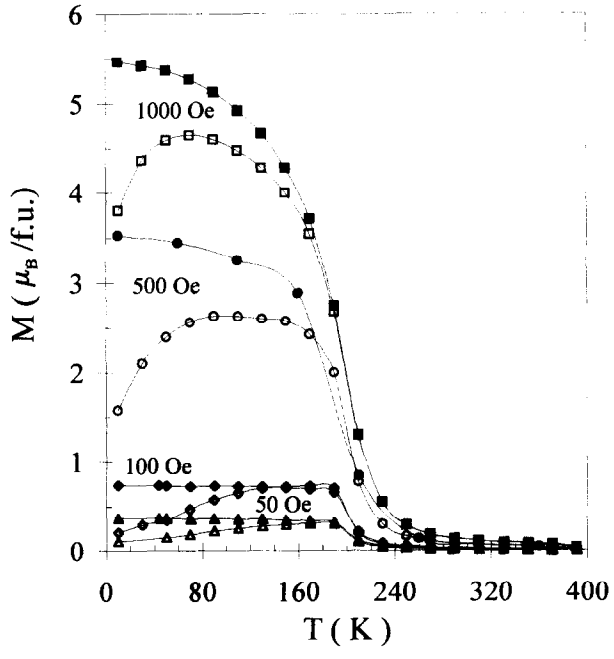

Fig. 3. Free-powder magnetization M of $UFe_{10}Mo_2$ under various magnetic fields as a function of temperature T: full symbols, field cooled; open symbols, zero-field cooled.

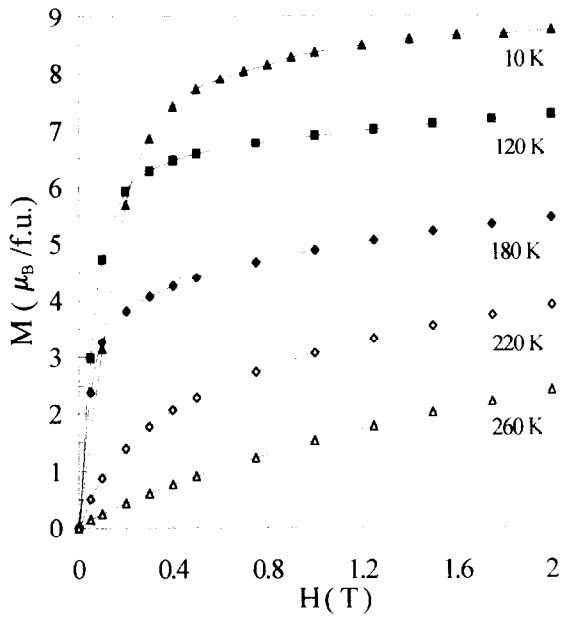

Fig. 4. Free-powder magnetization curves of $UFe_{10}Mo_2$ at various temperatures.

value of 8.8 μ_B/f.u. was obtained for the extrapolated magnetization $M_0(T \rightarrow 0)$.

Magnetization measurements were performed both on loose powder free to rotate in the applied field and on powder with particles fixed with solid paraffin. The magnetization dependence on temperature was identical in both cases. In the $M(H)$ curves an expected smaller slope was observed for the fixed powder at low fields and the magnetization values are lower for the same applied fields. In this case the value obtained from the high field linear dependence indicates a magnetization at $T=0$ of $M_0(T \rightarrow 0) \approx 6.6$ μ_B/f.u.

The comparison between these two values for the free and fixed powders (Fig. 5) gives an indication of the magnetic anisotropy type for this system. According to previous theoretical calculations for a highly anisotropic magnet [33], our value of $M_s^{fix}/M_s^{free} = 0.75$ suggests a basal plane character of the anisotropy similar to that for the $NdFe_{10}Mo_2$ isostructural compound [34]. An increase in this ratio occurs at the ferromagnetic transition temperature, the ratio becoming almost 1.0 at higher temperatures. These results are consistent with the idea that the ferromagnetic transition leads to a drastic decrease in the total anisotropy.

In the absence of neutron diffraction results and from the present experimental data alone it is difficult to assign the origin of the observed value of 8.8 μ_B/f.u. for the saturation magnetization at low temperature. This value is significantly smaller than that found for $YFe_{10}Mo_2$ ($T_c = 323$ K), for which $M_s(T=4.2$ K$) = 14.1$ μ_B/f.u. was obtained from magnetization measurements [35], in good agreement with the value of $M_s(T=4.2$ K$) = 14.68$ μ_B/f.u. [24] derived from Mössbauer spectra assuming $B_{hf} = 15.7$ T μ_B^{-1} [5]. In the present case, assuming $B_{hf} = 14.5$ T μ_B^{-1}, Mössbauer data indicate a value of 5.4 μ_B/f.u. at 80 K, which should be compared with the free-powder saturation magnetization of about 7 μ_B/f.u. at the same temperature. This comparison indicates that in addition to the Fe atoms remaining paramagnetic at low temperatures, the U atoms can have a non-negligible magnetic moment. We expect further experiments will resolve this question.

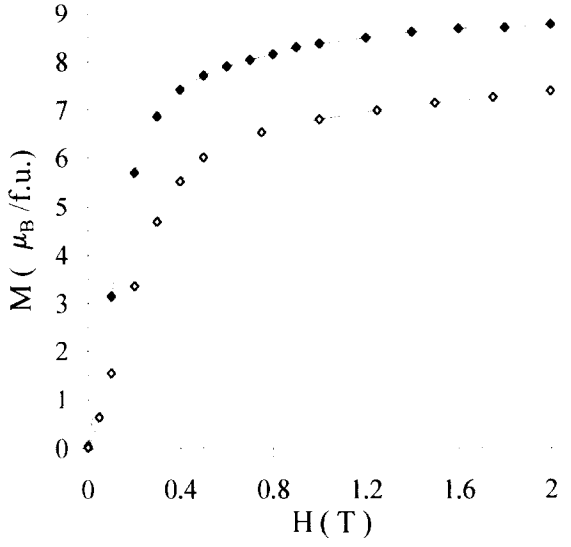

Fig. 5. Magnetization curves of $UFe_{10}Mo_2$ at 10 K: open symbols, fixed powder; full symbols, free powder.

Acknowledgements

The authors are thankful to Professors G.M. Kalvius and W. Potzel for illuminating discussions. This work was partially supported by Junta Nacional de Investigação Científica e Tecnológica (Portugal) through contract PBIC/FIS/634/93 and by NATO through Collaborative Research Grant 920996. Support given to J.C.W. in the frame of the EC-funded training programme "Human Capital and Mobility" is also acknowledged.

References

[1] A.V. Andreev, W. Suski, F.G. Vagizov and H. Drulis, *Physica B, 186–188* (1993) 730.

[2] W. Suski, A. Zaleski, D. Badurski, L. Folcik, K. Wochowski, B. Seidel, C. Geibel and F. Steglich, *J. Alloys Comp., 198* (1993) L5.

[3] S.F. Matar, B. Chevalier and J. Etourneau, *J. Magn. Magn. Mater.*, in press.

[4] J. Gal, I. Yaar, D. Regev, S. Fredo, G. Shani, E. Arbaboff, W. Potzel, K. Aggarwal, J.A. Pereda, G.M. Kalvius, F.J. Litterst, W. Schäfer and G. Will, *Phys. Rev. B, 42* (1990) 8507.

[5] H.S. Li and J.M.D. Coey, in K.H.J. Buschow (ed.), *Handbook of Magnetic Materials,* Vol. 6, North-Holland, Amsterdam, 1991, p. 1.
[6] K.H.J. Buschow, in G.J. Long and F. Grandjean (eds.), *Supermagnets, Hard Magnetic Materials,* Kluwer, Dordrecht, 1991, p. 49.
[7] W. Suski, A. Baran and T. Mydlarz, *Phys. Lett. A, 136* (1989) 89.
[8] A. Baran, M. Łukasiak, W. Suski, J. Suwalski, H. Figiel, J. Opila, K. Turek and T. Mydlarz, *J. Magn. Magn. Mater., 83* (1990) 262.
[9] M. Zeleny, M. Rotter, W. Suski, A. Baran and F. Zounová, *J. Magn. Magn. Mater., 98* (1991) 25.
[10] A.C.T. North, D.C. Phillips and F.S. Mathews, *Acta Crystallogr. A, 24* (1968) 351.
[11] J.O. Lundgren, Crystallographic computer programs, *Rep. UUIC-B13-04-05,* 1982 (Institute of Chemistry, University of Uppsala).
[12] J.A. Ibers and W.C. Hamilton (eds.), *International Tables for X-Ray Crystallography,* Vol. 4, *Revised and Supplementary Tables,* Kynoch, Birmingham, 1974.
[13] J.P. Becker and P. Coppens, *Acta Crystallogr. A, 30* (1974) 129.
[14] J.P. Becker and P. Coppens, *Acta Crystallogr. A, 31* (1975) 417.
[15] T. Hahn (ed.), *International Tables for Crystallography,* Vol. A, *Space Group Symmetry,* Reidel, Dordrecht, 1983.
[16] J.C. Waerenborgh and F. Teixeira de Queiroz, *LNETI, ICEN, Internal Rep.,* 1984.
[17] A.J. Stone, Appendix to G.M. Bancroft et al., *J. Chem. Soc. A,* (1967) 1966.
[18] D.B. De Mooij and K.H.J. Buschow, *J. Less-Common Met., 136* (1988) 207.
[19] F. Weigel, in J.J. Katz, G.T. Seaborg and L.R. Morss (eds.), *The Chemistry of the Actinide Elements,* Vol. 1, Chapman and Hall, London, 1986, p. 235.
[20] K.H.J. Buschow, P.C.P. Bouten and A.R. Miedema, *Rep. Prog. Phys., 45* (1982) 937.
[21] P.J. Spencer and F.H. Putland, *J. Chem. Thermodyn., 7* (1975) 531.
[22] W. Suski, F.G. Vagisov, H. Drulis, J. Janczak and K. Wochowski, *J. Magn. Magn. Mater., 117* (1992) 203.
[23] Th. Sinnemann, K. Erdmann, M. Rosenberg and K.H.J. Buschow, *Hyperf. Interact., 50* (1989) 675.
[24] C.J.M. Denissen, R. Coehoorn and K.H.J. Buschow, *J. Magn. Magn. Mater., 87* (1990) 51.
[25] Th. Sinnemann, M. Rosenberg and K.H.J. Buschow, *J. Less-Common Met., 146* (1989) 223.
[26] A.P. Gonçalves, J.C. Waerenborgh, G. Bonfait, A. Amaro, M.M. Godinho, M. Almeida and J.C. Spirlet, *J. Alloys Comp., 204* (1994) 59.
[27] T. Berlureau, B. Chevalier, P. Gravereau, L. Fournes and J. Etourneau, *J. Magn. Magn. Mater., 102* (1991) 166.
[28] B.-P. Hu, H.-S. Li, J.P. Gavigan and J.M.D. Coey, *J. Phys. Condens. Matter, 1* (1989) 755.
[29] B.-P. Hu, H.-S. Li and J.M.D. Coey, *Hyperf. Interact., 45* (1989) 233.
[30] Y.-C. Yang, H. Sun, L.-S. Kong, J.-L. Yang, Y.-F. Ding, B.-S. Zhang, C.-T. Ye, L. Jin and H.-M. Zhou, *J. Appl. Phys., 64* (1988) 5968.
[31] S.S. Jaswal, Y.G. Ren and D.J. Sellmeyer, *J. Appl. Phys., 67* (1990) 4564.
[32] R. Coehoorn, *Phys. Rev. B, 41* (1990) 11 790.
[33] A.V. Andreev, H. Nakotte and F.R. de Boer, *J. Alloys Comp., 182* (1992) 55.
[34] L. Schultz and J. Wecker, *J. Appl. Phys., 64* (1988) 5711.
[35] H. Sun, M. Akayama, K. Tatami and H. Fujii, *Physica B, 183* (1993) 33.